# Photooxidation of Anhydride-Cured Epoxies: FTIR Study of the Modifications of the Chemical Structure

**V. OLLIER-DUREAULT,[1] B. GOSSE[2]**

[1] Schneider Electric, Materials Research Division, Site A3, 38050 Grenoble Cedex 9, France

[2] CNRS–LEMD, 25 rue des Martyrs, 38040 Grenoble Cedex 9, France

*Received 5 August 1997; accepted 6 April 1998*

**ABSTRACT:** Anhydride-cured epoxies are used in electrical engineering to manufacture insulators. The purpose of this study is to determine the modifications undergone by these resins when exposed to solar-type radiation (radiation with a wavelength of more than 300 nm). Two epoxy–anhydride systems have been studied. Using transmission Fourier transform infrared (FTIR) and attenuated total reflection (ATR), we have determined the structural modifications and the groups formed during photooxidation. The degradation is very heterogeneous, more significant on the surface than in the bulk of the material, and a considerable decrease in almost all the initial functional groups is observed. The flexibilized system, richer in ester groups but containing fewer phenyl groups, degrades more rapidly during the first hours of exposure than the nonflexibilized system. Two explanations accounting for this faster degradation in the first hours of exposure are drawn from ultraviolet absorbance analysis and degradation mechanisms considerations. After 40 h of irradiation, the disappearance rate of the aromatic groups depends only on their initial concentration, whereas the formation kinetics for the hydroxyl groups is limited by the diffusion of oxygen in the material. Chemical treatments using $SF_4$, $NH_3$, and NaCl have revealed the formation of hydrophilic products, acids, and alcohols. Their presence and particularly high concentration at the surface could very well be responsible for the degradation of the insulating properties of the electrical insulators.  J Appl Polym Sci 70: 1221–1237, 1998

**Key words:** epoxy–anhydride resins; photodegradation; FTIR spectroscopy; aging of insulators; hydrophilic surface

## INTRODUCTION

Cast epoxy resins based on di-glycidyl ether of Bisphenol A (DGEBA) are widely used in electrical engineering to manufacture indoor insulators. Such insulators can undergo an oxidative surface attack by ultraviolet radiation, for instance, when exposed to sunlight during transport or when electrical discharges occur.

The purpose of this study is to analyze structural modifications in 2 DGEBA-based epoxy–anhydride systems during photooxidation by ultraviolet (UV) radiation in the solar wavelength range and to analyze the degradation products. A third epoxy–anhydride system based on a cycloaliphatic epoxide will be studied for comparison purpose.

As far as we know, there has been no previous work on the photodegradation of DGEBA based epoxy–anhydride systems in air. On the other hand, a number of studies have dealt with the thermal or photochemical degradation of phenoxy resins,[1,2] noncrosslinked DGEBA resins,[3] and, es-

*Correspondence to:* B. Gosse.

Journal of Applied Polymer Science, Vol. 70, 1221–1237 (1998)
 CCC 0021-8995/98/061221-17

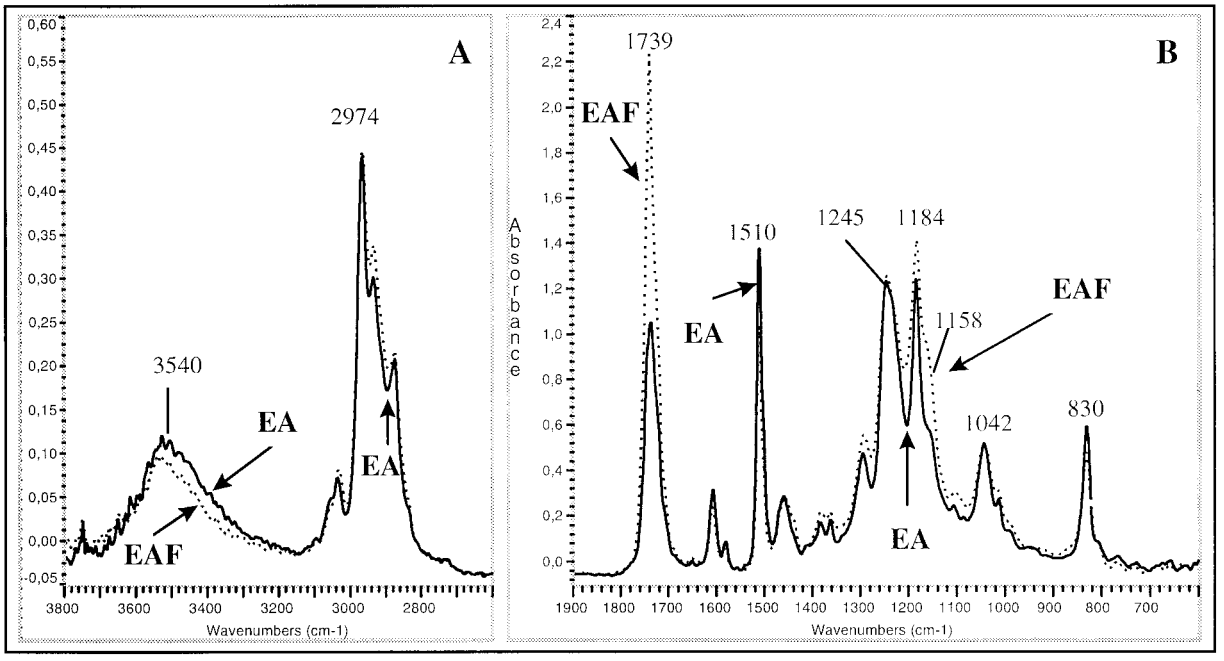


**Figure 1** FTIR spectra of the EA (——) and EAF (. . .) systems.

pecially, epoxy resins crosslinked by amines. For the latter, refer to the article by Lin et al.,[4] which contains numerous references, or the more recent work of Bellenger and Verdu[5] on the influence of the chemical structure on the photooxidation of epoxy–amine systems. The work of Le Huy et al.[6,7] concerns the thermooxidative degradation of epoxy–anhydride systems, while that of Lin et al.[4] concerns an Fourier transform infrared (FTIR) study of the thermal and photochemical degradation of epoxy systems crosslinked by trimethoxyboroxine. Finally, relatively recent studies[8,9] on the pyrolysis of epoxy resins crosslinked by different hardeners, including anhydrides, constitute further references on the relative thermal stability of the different structural groups of these systems.

In the present work, we propose a structural representation of the 2 DGEBA-based epoxy systems that accounts for the major differences between the 2 formulations, as observed by Fourier transform infrared (FTIR) spectroscopy. Next, we present the FTIR analysis of the structural modifications produced and the products formed when these materials are exposed to UV radiation. We particularly investigate the quantities and the distribution of the hydrophilic products, acids, and alcohols, their presence and concentrations on the surface being largely responsible for the degradation of the insulating properties of electrical insulators.

## EXPERIMENTAL

### Materials

The 2 studied formulations, referred to as the EA (epoxy–anhydride) and EAF (flexibilized epoxy–anhydride) systems, respectively, are commercial formulations composed of a DGEBA-type epoxy resin, an anhydride hardener based on methyl tetrahydrophtalic anhydride (MTHPA), and a catalyst of the tertiary amine-type. The EAF system further contains a diester–dicarboxylic acid flexibilizer. The cycloaliphatic system studied for comparison, referred to as the EAC system, is also a commercial formulation composed of a cycloaliphatic epoxy resin and an anhydride hardener based on HHPA (hexahydrophtalic anhydride). It is thus aromatic free.

Analysis by gel permeation chromatography (GPC) and by FTIR spectroscopy of the basic constituents and subsequently of the crosslinked systems (Fig. 1) have led us to the following conclusions for the aromatic systems.

The EA system is made up of a mixture of DGEBA oligomers that can be assimilated with DGEBA $n = 1.5$ (long chains), crosslinked by MTHPA. The constitutional repeating half-unit (CRU) is represented in Figure 2(A).

The EAF system is made up of a mixture of DGEBA oligomers with $n = 0$ and 2, crosslinked

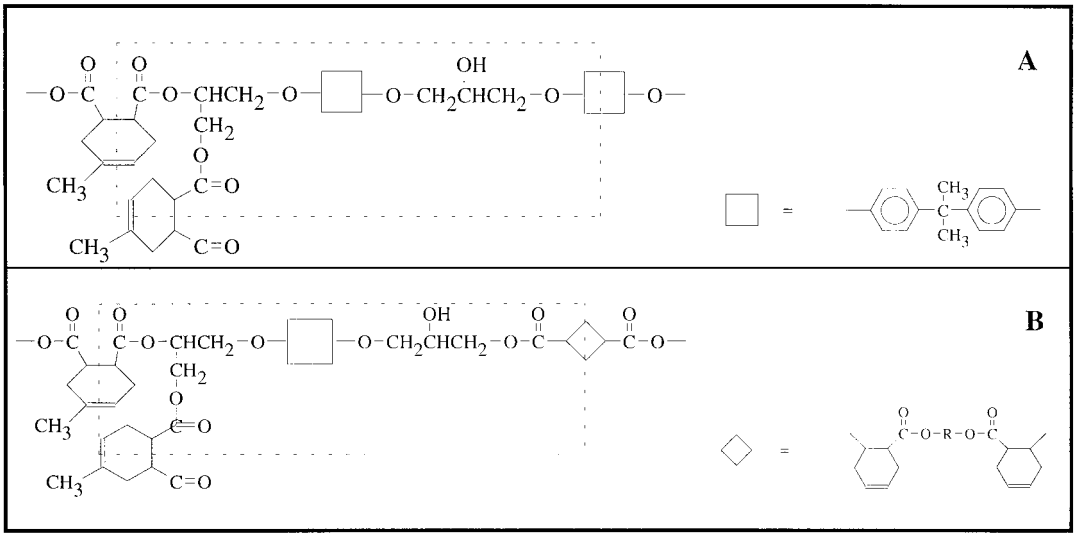


**Figure 2** (A) Constitutional repeating half-unit of the EA network. (B) Constitutional repeating half-unit of the EAF network characteristic of this system and accounting for 40% (w/w) of the material.

by the MTHPA anhydride after an initial step involving the elongation of the DGEBA $n = 0$ chains (short chains) by a tetrahydrophtalic di-acid–diester type flexibilizer. Thus, 3 CRUs are necessary to describe the EAF system. The first is identical to that of the EA system [Fig. 2(A)] and corresponds to the reaction of the MTHPA anhydride with the DGEBA $n = 2$ di-epoxides. The second, shown in Figure 2(B), corresponds to the reaction of MTHPA with the di-epoxide molecules that have been elongated by the flexibilizer. Finally, the third CRU corresponds to the reaction of MTHPA with the DGEBA $n = 0$ di-epoxide molecules that have not reacted with the flexibilizer. The proportions of these 3 CRUs are 20, 40, and 40% by mass, respectively.

The ratio of identical groups per mass unit in the EA system [or functional index $IF_{EA}(X)$] versus that of the EAF system [$IF_{EAF}(X)$] is given in Table I. It appears that the EA system contains

**Table I Attribution of the IR Bands of the 2 Crosslinked Systems and the Calculated Ratios of Functional Indices in the 2 Systems**

| | | Ratios of Functional Indices $IF_{EA}(X)/IF_{EAF}(X)$ | |
|---|---|---|---|
| Functional Groups | Wavelength Number ($cm^{-1}$) | Calculated Ratios (from CRU) | Absorbance Ratios |
| Hydroxyle (—OH) | 3520 | 1,54 | 1,43 |
| Arylene (C—H) | 3052, 3033 | 1,34 | 1,31 |
| Methyl (CH3) | 2966, 2872 | 1,07 | 1,04 |
| Methylene (CH2) | 2931 | 0,97 | 0,93 |
| Dimethyl —C(CH3)2 | 1381, 1363,807 | | |
| Phenylene (C═C) | 1610, 1580, 1510, | 1,43 | 1,4 |
| Phenyl ortho di-substituted | 1458 | | |
| Phenyl—C(CH3)2—Phenyl | 1184 | | |
| p-phenylene | 830 | | |
| Ester (OC═O) | 1739, 1152 | 0,68 | 0,68 |
| aromatic Ether Φ—O—C | 1240 | 1,38 | 1,48 |
| aliphatic Ether Φ—O—C | 1042 | | |

**Table II Procedure for the Preparation of Cast Test Pieces From Which 10-$\mu$ Films Are Cut Using a Microtome**

| Operations | System EA | System EAF |
|---|---|---|
| Preparation of the mixture | 40°C | 130°C |
| Degassing under vacuum | Few minutes | |
| Casting | In the preheated mold at the curing temperature | |
| Curing (duration : 3 × gel-time) | 140°C | 130°C |
| Demolding | Before cooling | |
| Postcuring | 140°C, 8-h duration | |

1.5 times more aromatic groups than the EAF system, whereas the percentage for ester groups is approximately 1.5 times lower.

The cycloaliphatic epoxy–anhydride (CEA) is made up of di-glycidyl ether of cyclohexane crosslinked by hexa-hydrophtalic-anhydride (HHPA).

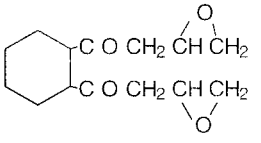

di-glycidyl-ether of cyclohexane

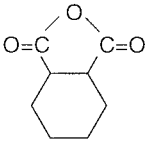

HHPA

For the entire study, except for the determination of oxydation profiles, the samples are films about 10 $\mu$ thick, cut using a microtome (universal motorized JUNG Autocut 2055, LEICA) from the center of test pieces cast under atmospheric pressure in air. For the determination of oxydation profiles, those test pieces, previously aged under UV irradiation, are cut from surface to center to get a 10-$\mu$ thick film allowing microscopic FTIR mapping (by transmission) 20 by 20 $\mu$ starting from the surface edge. Table II gives the procedure used for the preparation of these cylindrical test pieces (6 mm height and 35 mm diameter). The proportions of resin and hardener used are those recommended by the supplier and correspond to the stoichiometric mixture. The quantity of accelerator added in the case of the EA system is 0.2% by weight with respect to the epoxy resin. For the EAF system, the accelerator is included in the resin and the flexibilizer in the hardener.

The difference in preparation temperatures is due to the fact that the resin in the EA system is a solid at room temperature and must be heated before mixing, whereas the resin in the EAF system is already a liquid at room temperature. In addition, the difference in curing temperatures makes it possible to compensate for the difference in reactivities and to ensure an identical jellification time, about 18 min, for the 2 systems.

### Aging Apparatus

The apparatus used for the aging process is a closed 40-L chamber with 3 overhead high-pressure mercury arc lamps (OSRAM Ultravitalux 300 W). The samples are placed at a distance of 25 cm from the lamps on a revolving plate, thus ensuring identical irradiation of all the samples. In order to filter the IR radiation and to limit thermodegradation as compared to photodegradation, an IR filter is placed between the lamps and the samples. With the lamps turned on, the tem-

**Table III Measurements of Energy Densities Received at the Surface of the Samples**

| Spectral Region Centered on Energy Densities | 254 nm | 310 nm | 365 nm |
|---|---|---|---|
| Lamps placed at a distance of 25 cm | 0.7 W/m$^2$ | 5.5 W/m$^2$ | 20 W/m$^2$ |
| In Grenoble at summertime in the midday sun | 0.8 W/m$^2$ | 6.4 W/m$^2$ | 23,6 W/m$^2$ |

perature in the chamber during degradation is 60°C. Also owing to the IR filter, the differences in surface temperatures between samples with different IR absorptions may be disregarded. In addition, the variation of the energy density with the wavelength was checked using an UV radiometer (ORIEL UVX) equipped with filters centered on 3 wavelengths characteristic of mercury arc lamps: 254, 310, and 365 nm (Table III). The values measured in Grenoble in summer, at ground level, at noon, in the sun and centered on the same wavelength are very similar (Table III). We have checked that the structural modifications caused by irradiation in this laboratory chamber are representative of those caused by an natural outdoor exposure.

### Methods of Characterizing the Aging

FTIR transmission microscopy was used to observe the structural evolution of the 10-$\mu$ thick films during degradation. The employed apparatus was a Nicolet 510 equipped with a Spectratech IR-plan microscope.

The IR bands (Table I) were attributed using reference works,[10–12] the results of Lin et al.,[4] and especially those of Stevens,[13,14] and by comparing the spectra of the constituents with those of the 2 crosslinked systems (Fig. 1).

### Methods of Analyzing the Photoproducts

The degradation products, and, more specifically, the carboxylic acids and alcohols, were identified by combining the FTIR spectroscopy with specific chemical reactions, allowing certain IR bands to be shifted towards less crowded regions of the spectrum.

Thus, gaseous $SF_4$ reacts with acids, alcohols, and hydroperoxides according to the following scheme[15,16]:

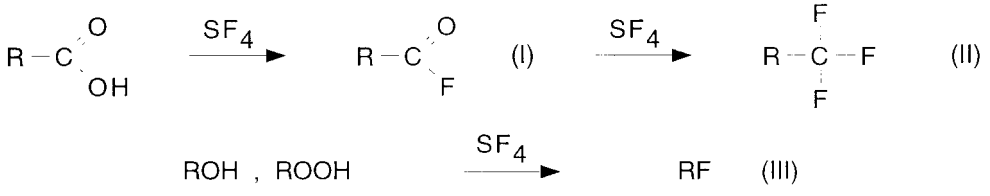


After treatment, the bands characteristic of acids [mainly $\nu$OH around 3300 $cm^{-1}$, overtones and combinations of carboxylic acid dimers around 2600 $cm^{-1}$,[12] $\nu$C═O intense band around 1710 $cm^{-1}$, and $\nu$C—O strong band between 1315 and 1280 $cm^{-1}$] should disappear, leaving room for the absorption bands characteristic of the corresponding fluorinated derivatives. In particular, the $\nu$C═O band of acyl fluorides (I) should appear between 1850 and 1800 $cm^{-1}$, and its gradual transformation into $RCF_3$.[17] Likewise, the bands characteristic of alcohols or hydroperoxides ($\nu$OH at 3450 $cm^{-1}$) should disappear, leaving room for the absorption bands characteristic of the corresponding monofluorinated compounds (around 1080 $cm^{-1}$). Pure aldehydes or ketones can react with $SF_4$; however, inside a polymeric matrix, they do not generally react when the treatment takes place at room temperature.[16] The absence of reaction with esters was confirmed.

Gaseous $NH_3$ reacts with carboxylic acids according to a classical acid–base reaction to yield the corresponding ammonium and carboxylate ions:


This reaction should therefore lead to the disappearance of the bands characteristic of acids (3300, 2600, and 1700 $cm^{-1}$) and the appearance of bands characteristic of ammonium ions ($\nu$CH around 3200 $cm^{-1}$) and carboxylate ions (asymmetrical $\nu$C═O between 1550 and 1600 $cm^{-1}$ and symmetrical $\nu$C═O between 1300 and 1400 $cm^{-1}$).[16] $NH_3$ may also react with esters or anhydrides to yield amides, the absorption of which appears around 1665 $cm^{-1}$.[17] Finally, by carrying out an acid return with HCl (vapors), the carboxylate ions immediately reform the carboxylic acid.[17,18]

$NH_3$ in the gaseous state does not react with alcohols, nor with aldehydes or ketones. We have verified that it does not react with esters under our operating conditions by treating unirradiated films with $NH_3$.

However, assuming the possible faculty of $NH_3$ to favor the formation of carboxylic acid by hydrolysis of esters on oxidized and, thus, hydrated surfaces, a second chemical treatment characteristic of acids was employed, using sodium chloride NaCl. Indeed, NaCl may react by ion exchange with ions in the matrix according to the reaction:

$$Na^+Cl^- + RCOO^-H^+ \rightarrow RCOO^-Na^+ + H^+Cl^-$$

The hydrochloric acid HCl, in turn, is then able to react, but its presence requires a previous exchange between the $Na^+$ and the $H^+$ stemming from the oxidized polymer.

In addition, FTIR microscopy by attenuated total reflectance (ATR), with which the acquisition of a spectrum is achieved with a single reflection on the surface, was used to compare the surface (at a depth of about a micron) and bulk compositions of the aged films. Finally, the UV absorbance of the photoproducts was determined by UV absorption spectroscopy.

## RESULTS AND DISCUSSION

### Modification of the Chemical Structure

#### *Analysis by Transmission FTIR*

The FTIR analysis as a function of the irradiation time (1 spectrum every 10 h from 0 to 100 h, then every 24 h until 180 h, and, finally, a spectrum at 240 h) shows a rapid spectral evolution of the 2 systems under UV radiation, which can be observed from the very first hours of exposure, as illustrated in Figure 3, as follows.

- A major decrease of the bands characteristic of aromatics is shown (para-disubstituted, aromatic C═C bands at 1610 and 1510 $cm^{-1}$, aromatic CH bands at 3032 and 830 $cm^{-1}$) [Fig. 3(A) and (C)].
- A decrease of the ether groups (band at 1042 $cm^{-1}$) associated with a decrease of the aromatic ether band (band at 1245 $cm^{-1}$), [Fig. 3(C)] is shown.
- A decrease of the aliphatics [$C(CH_3)_2$ band at 1184 $cm^{-1}$, $(CH_3)_2$) band at 807 $cm^{-1}$, $CH_3$ bands at 2966 and 2874 $cm^{-1}$, and $CH_2$ band at 2933 $cm^{-1}$] is shown [Fig. 3(A) and (C)].
- A strong increase of the hydroxyls (shoulder at 3600 $cm^{-1}$ and maximum at 3450 $cm^{-1}$) gradually yielding more tightly bound hydroxyls (shoulder at about 3250 $cm^{-1}$ and a broad band around 2600 $cm^{-1}$) is shown [Figures 3(A) and 10]. The increase in the OH band varies linearly with the irradiation time until approximately 30 to 40 h. After 40 h, the increase varies as a function of $t^{0.5}$ (Fig. 4). It is generally accepted that such a variation indicates an oxidation process limited by the diffusion of oxygen in the polymer.[7] It results in a heterogeneous volume distribution of the material's oxidation products in thick samples, as is shown in Figure 5.
- The appearance of several carbonyl and carboxyl groups absorbing in the range of 1800 to 1680 $cm^{-1}$ is shown, which may be attributed to lactones or peroxyesters (1800–1760 $cm^{-1}$) and ketones or carboxylic acids (1720–1680 $cm^{-1}$) [Figure 3(B)].

For the EAF system, which is rich in ester groups, we note a particularly fast and significant disappearance of the C═O and C—O bands of esters between 0 and 50 h (Fig. 6). An identical decrease of all the other bands is associated with these modifications, such as, for instance, that of the aromatic groups at 830 $cm^{-1}$ (Fig. 7). After 50 h, the EA and EAF systems degrade according to an apparent first-order reaction and with an identical rate. After 240 h of irradiation, the intensity of the aromatic bands has decreased by over 40%.

Note that it was not possible to take into account the possible loss of matter due to the formation of volatile products. The decrease of all bands, including that of the aromatic band at 1610 $cm^{-1}$, which was chosen as a reference for thermodegradation,[7] forced us to work with films of a given thickness, which we had to assume constant throughout the aging process.

The modification or disappearance of numerous absorption bands, associated with the strong increase of the hydroxyl band and the broadening of the carbonyl band, is evidence of an important oxidation phenomenon in both systems. As for the attacks that are common to both formulations, the obtained results show that UV irradiation leads to a specific attack upon (1) the aromatic functions [disappearance of aromatic C═C and C—H bands], and (2) the aliphatic functions located near aromatic centers in the chain [disap-

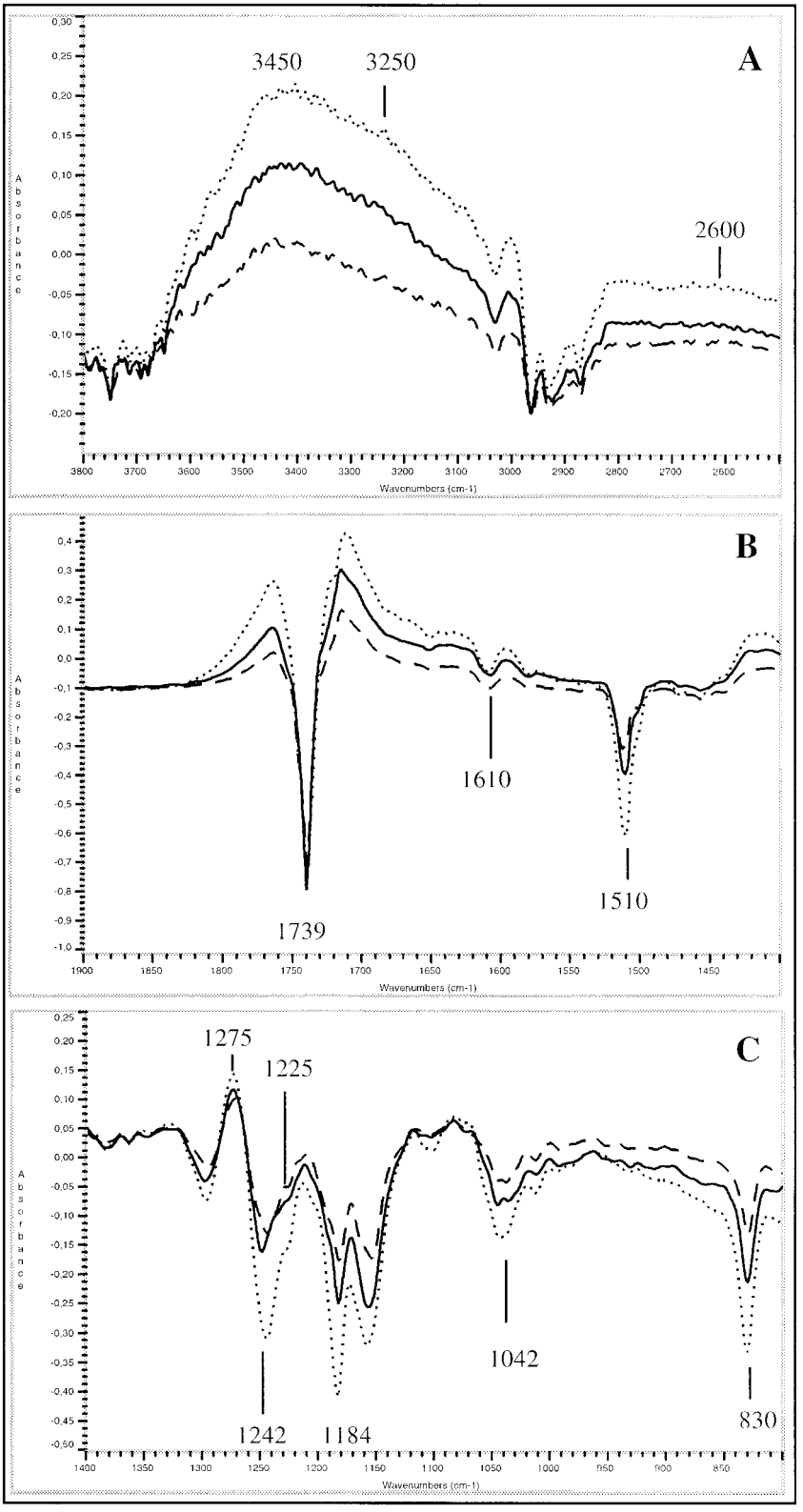


**Figure 3** Subtracted IR spectra between a new EAF sample and an irradiated one. Irradiation time: 52 (---), 102 (——), and 240 (. . .) h.

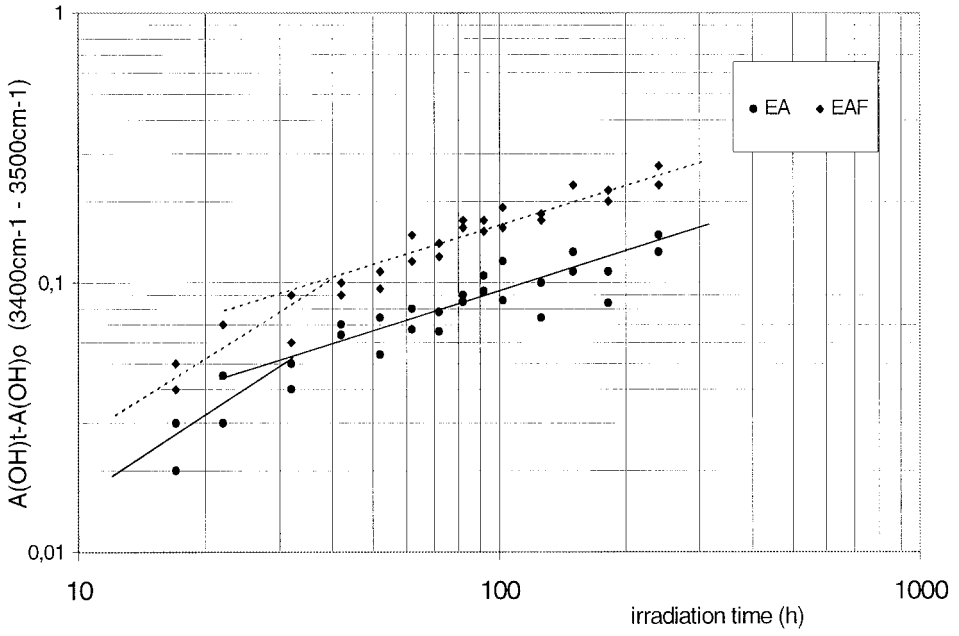


**Figure 4** Absorbance of the OH groups (taken at the maximum) as a function of the irradiation time: EA (——); EAF (---).

pearance of the aliphatic ether bands, decrease of the aromatic ether band, the —$C(CH_3)_2$, the $CH_2$, and $CH_3$ bands]. In addition, it may be possible that the aliphatic groups, which are slightly further from these aromatic centers, may also be attacked, but the corresponding bands are very difficult to observe by IR (this is the case for tertiary CH groups, notably those with a very low molecular absorption coefficient $\varepsilon$, as well as the secondary alcohols, for which the absorption band is overlapped by the others).

For the EAF system, a rapid attack upon all groups, and, particularly the esters, takes place at the beginning of the degradation (Fig. 6). At the same time, we note a rapid disappearance of a band at 665 $cm^{-1}$ corresponding to the cis-dialkyl vinyl group of the flexibilizer's tetrahydrophtalic diacid–diester. Based on the presented structural models, the quantity of ester groups belonging to the flexibilizer in the EAF system (21%) is of the same order of magnitude as the percentage of degradation of ester groups in the EAF system, as measured at 50 h (approx. 28%). These observations suggest a rapid attack of the flexibilizer, which possesses ester groups of a different configuration than those common to the 2 systems. In addition, they are located near the network nodes and are therefore particularly fragile. Once the flexibilizer has been consumed, the EAF systems continues to degrade. The disappearance of the aromatics then follows the same kinetics for both systems (Fig. 7).

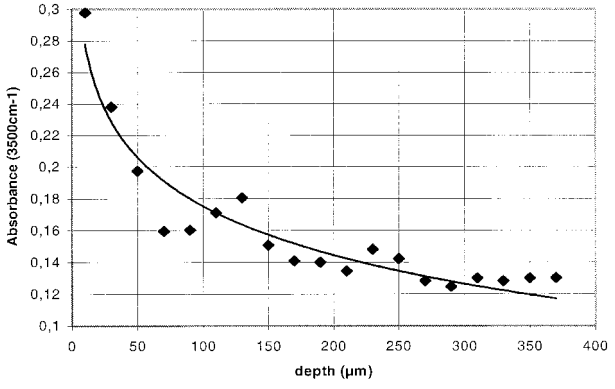


**Figure 5** Oxidation profile in a thick sample: absorbance at 3500 $cm^{-1}$ as a function of the distance to the irradiated face (EAF system; 200-h irradiation time).

### *Identification of the Photoproducts*

Polymers that have undergone a thermal or photochemical aging process in the presence of oxygen generally give rise to a complex mixture of the following oxidation products: alcohols, hydroperoxides, ketones, aldehydes, carboxylic acids, esters, peracids, peroxyesters, and anhydrides. As a matter of fact, we observe the appearance of new absorption bands in regions that are characteris-

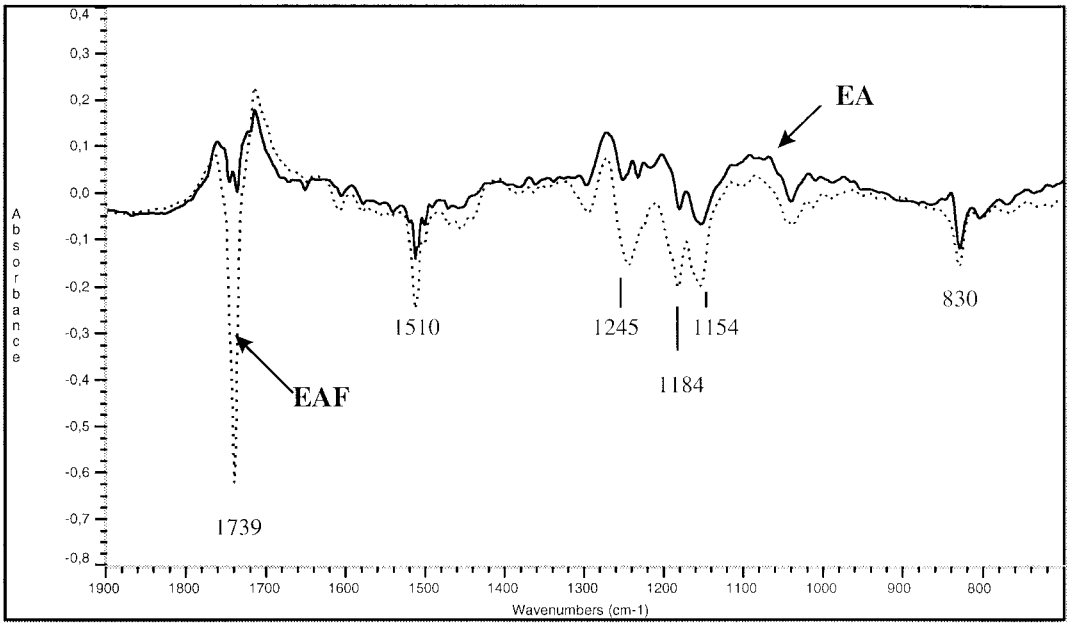


**Figure 6** Subtracted IR spectra between a new sample and a sample irradiated for 102 h: EA (——); EAF (. . .).

tic of hydroxyls, carbonyls and ethers (Fig. 3). These bands are often very broad and result from the overlapping of bands that are characteristic of several photoproducts, as follows:

- The hydroxyl OH region, with several bands (3600, 3465, 3250, and 2600 $cm^{-1}$) that may correspond to alcohols, phenols, hydroperoxides, or carboxylic acids [Fig. 3(A)];

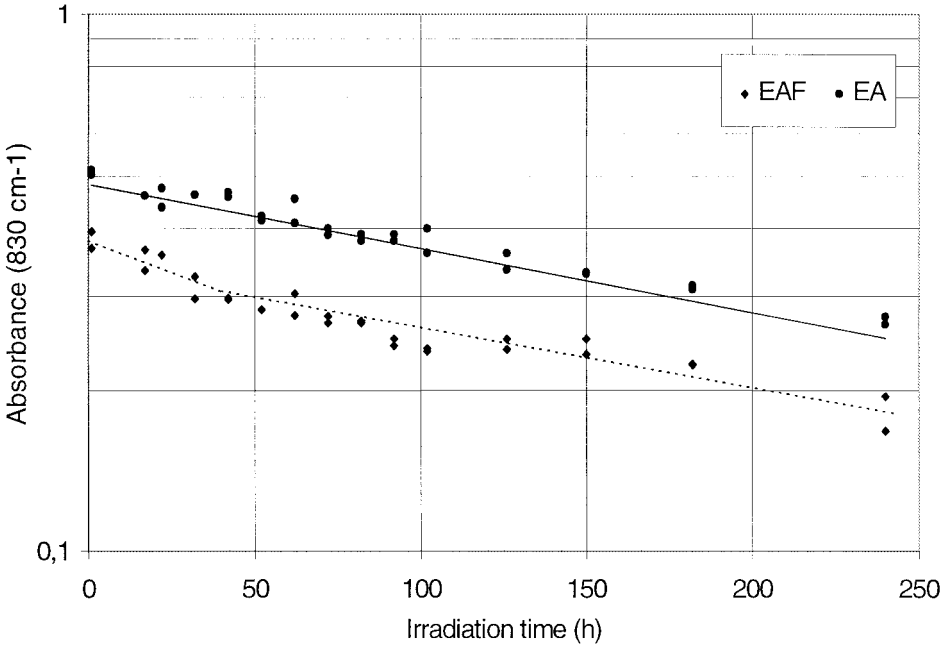


**Figure 7** Decrease of the aromatic IR band versus irradiation time for an EA (——) and EAF (---) system.

- The carbonyl C═O region, with several maxima or shoulders [Fig. 3(B)], 1764 $cm^{-1}$ (lactones or peroxyesters), 1715 $cm^{-1}$ (ketones or carboxylic acids), 1787 $cm^{-1}$ (acid anhydrides), 1724 $cm^{-1}$ (aldehydes), 1704 $cm^{-1}$ (carboxylic acids), and 1690 $cm^{-1}$ (conjugated ketones or benzoic acid);
- C—O region, with a main band at 1275 $cm^{-1}$, a shoulder around 1225 $cm^{-1}$, and an upsurge in the 1000–1100 $cm^{-1}$ range that may correspond to the C—O vibrations of carboxylic acids, phenols, alcohols, or ethers [Fig. 3(C)].

All of these new bands are common to both the EA and the EAF system but are different from those observed by Le Huy et al.[7] for thermodegradation. In this study, the major products were anhydrides, which may be identified by a characteristic doublet at 1850 and 1785 $cm^{-1}$, whereas we only observe a small shoulder at 1787 $cm^{-1}$ and a very weak band at 1850 $cm^{-1}$. Thus, it is clear that these are not the major products in the case of photodegradation. The following was observed.

- The reaction with gaseous $SF_4$ (Fig. 8) provokes the disappearance of the broad hydroxyl band between 3700 and 3000 $cm^{-1}$ [Fig. 8(A)] and the appearance of several bands corresponding to fluorinated alkyls in the 1000 to 1100 $cm^{-1}$ range [Fig. 8(C)]. These observations lead us to the conclusion that alcohols are present in the oxidized polymer in a rather high proportion. The RF products seem rather unstable or volatile since a notable fluctuation is observed in the corresponding bands as a function of the duration of treatment. The decrease of the C═O band between 1690 and 1725 $cm^{-1}$, associated with the appearance of fluorinated derivatives absorbing around 1850 and 1800 $cm^{-1}$, proves the presence of carboxylic acids in a relatively low concentration. Indeed, the intensity of the decrease of the acid bands as well as that of the increase of the corresponding fluorinated derivatives remains rather low. In addition, we observe the decrease of the carbonyl C═O band at 1739 $cm^{-1}$ [Fig. 8(B)]. This might be explained by a very slow reaction between $SF_4$ and the polymer's ester functions. The reaction is not observed with unaged polymer but would be made possible by the general degradation of the polymer. Finally, the bands appearing at 1262 $cm^{-1}$ and between 800 and 900 $cm^{-1}$ [Fig. 8(C)] are attributed either to $RF_3$ products (ultimate derivatives of the fluorinated acids), or more probably to fluorinated benzene groups, which might result from the action of $SF_4$ on phenols.
- The evolution observed due to the action of $NH_3$ (Fig. 9) confirms the presence of carboxylic acids in small quantities; in this case, an appearance between 1550 and 1590 $cm^{-1}$ of shoulders on the aromatic band at 1610 $cm^{-1}$ is observed, which is characteristic of carboxylate ions, associated with the disappearance of the shoulder around 1710 $cm^{-1}$. Meanwhile, the treatment leads to a decrease of almost all the bands of the initial spectrum of the aged film, a phenomenon which we attribute to the formation of a strongly absorbent superficial layer resulting from the reaction of $NH_3$ with the degradation products present at a high concentration at the surface of the film. After treatment with HCl, followed by a rinsing with distilled water, the resulting spectrum is comparable to the one obtained before treatment with $NH_3$; only the bands corresponding to products having reacted with $NH_3$ and eliminated by rinsing with distilled water have disappeared.
- Finally, the treatment with NaCl (assumed to exchange $Na^+$ with $H^+$ of carboxylic acid) has given an IR evolution that is very difficult to interpret as a whole (decrease of the carbonyls at 1750 and 1730 $cm^{-1}$ and increase of the hydroxyls); but the appearance of two bands characteristic of carboxylate ions (1575 $cm^{-1}$ and approximately 1400 $cm^{-1}$), associated with the disappearance of the carboxylic acid band at 1710 $cm^{-1}$ obtained by a simple ion exchange, confirms the presence of carboxylic acids in the oxidized polymer.

These results as a whole show that the UV irradiation of epoxy–anhydride resins must lead to a disappearance of material due to the formation of volatile molecules (CO, $CO_2$, $H_2O$, aromatic products of low molecular mass, etc.) not detected in this study. In addition, the following compounds are formed in relatively small quantities: (1) aliphatic alcohols, to which we attribute the OH band at 3450 $cm^{-1}$, the corresponding C—O band at 1080 $cm^{-1}$ and the different absorptions around 1000 $cm^{-1}$; (2) phenols, to which we

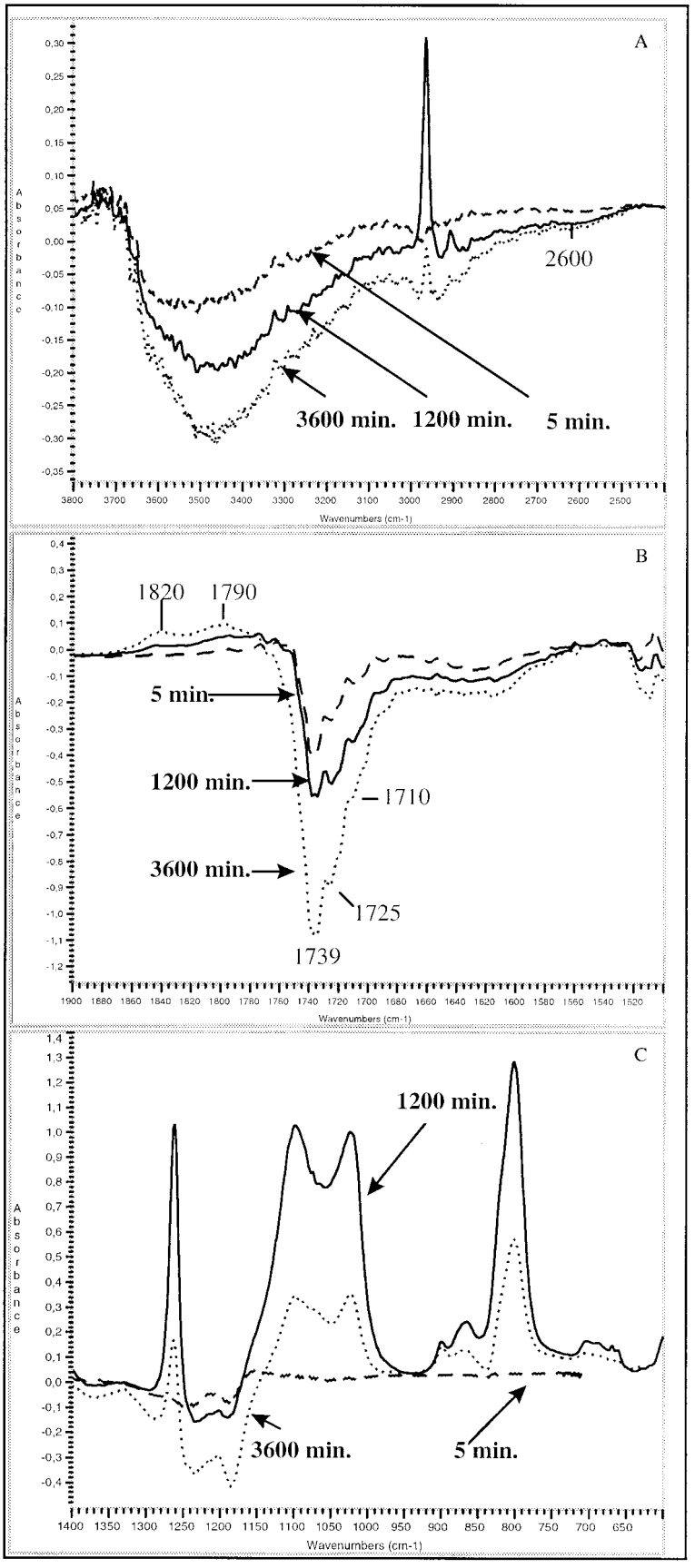


**Figure 8** Subtracted spectra between a sample irradiated for 100 h and the same sample treated with $SF_4$. Treatment time: 5 (---), 1200 (——), and 3600 (. . .) min.

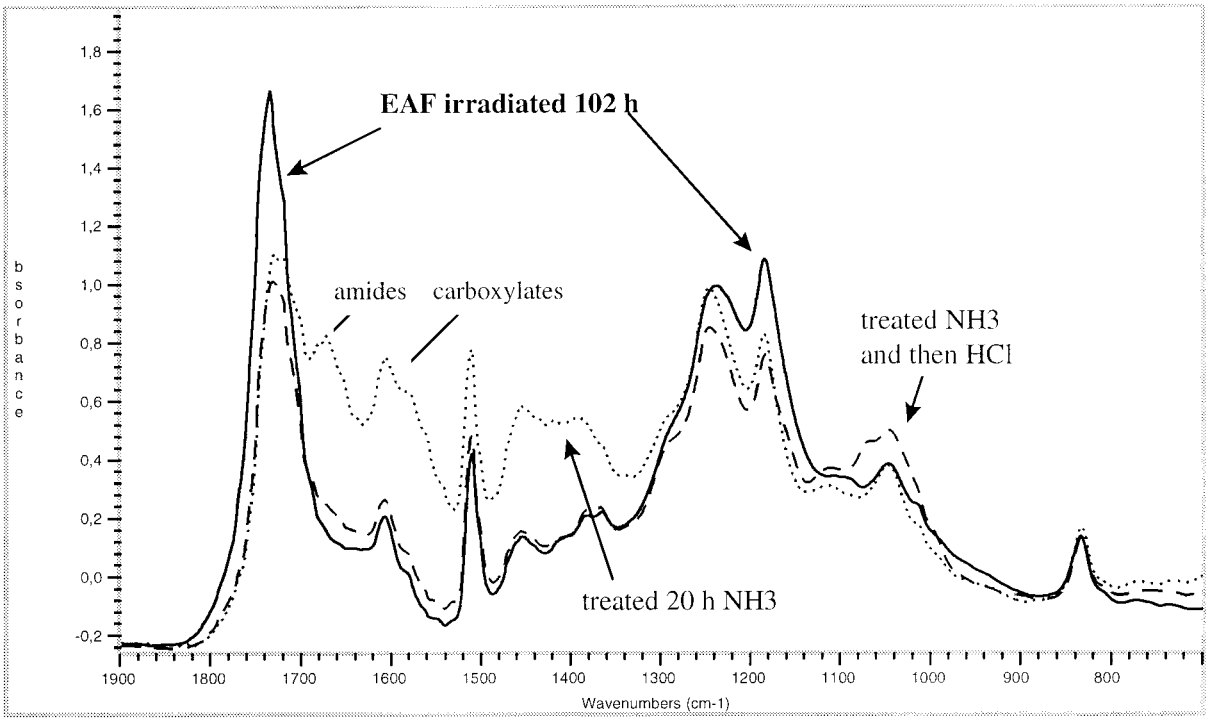


**Figure 9** IR spectra of an EAF sample irradiated for 102 h (——), then treated for 20 h with $NH_3$ (. . .), and finally exposed to HCl vapors, followed by rinsing with distilled water (— — —).

attribute the intense absorption bands at 3300 (OH), 1225 (C—C—O), and 1420 $cm^{-1}$ (C—OH)[12]; and (3) carboxylic acids, to which we attribute the C═O bands at 1700 and 1710 $cm^{-1}$, as well as the C—O band at 1275 $cm^{-1}$, the broad hydroxyl band between 2600 and 2900 $cm^{-1}$, and the absorption band around 950 $cm^{-1}$ (OH—O interaction).

Concerning the other products, we suggest the presence of saturated ketones (1724 $cm^{-1}$) and conjugated ketones (1690 $cm^{-1}$) or benzoic acid, as well as lactones (1764 $cm^{-1}$). In addition, a small quantity of anhydrides is observed around 1787 and 1820 $cm^{-1}$, but in relatively low concentrations, indicating that the photooxidation leads to the formation of different products from those of the thermooxidation.

The classical photooxidation processes, such as the molecular cleavage mechanisms of the Norrish I or II type, may be invoked in order to explain the formation of most of the observed groups. Part of the radicals that are formed during cleavage undergo a decarboxylation or a decarbonylation and successive cleavage, leading to the formation of a low-molecular-weight and, thus, volatile species.

### *Analysis of the Surface by ATR Microscopy*

The penetration of the degradation inside the bulk of the polymer depends on several factors, as follows: its absorbance in the considered spectral region; the possibility of the formation of absorbing photoproducts at the surface; and, a last important parameter, its permeability to oxygen. This is the reason why the degradation is often confined to the surface.

In order to determine the chemical composition at the extreme surface of the films, which may thus be different from the one detected by the technique of transmission FTIR, we have carried out an analysis by ATR microscopy of the side of the film that was exposed to the UV radiation. The spectra obtained by ATR for a 50-$\mu$ film irradiated for 160 h are shown in Figure 10. The spectrum obtained for the aged film has been multiplied by a factor 1.5.

Compared to the ATR spectrum of the new film, the ATR spectrum of the aged film shows a general decrease of all the initial bands. This decrease, which had already been observed by FTIR transmission reveals a strong surface degradation of the polymer (increase in roughness,

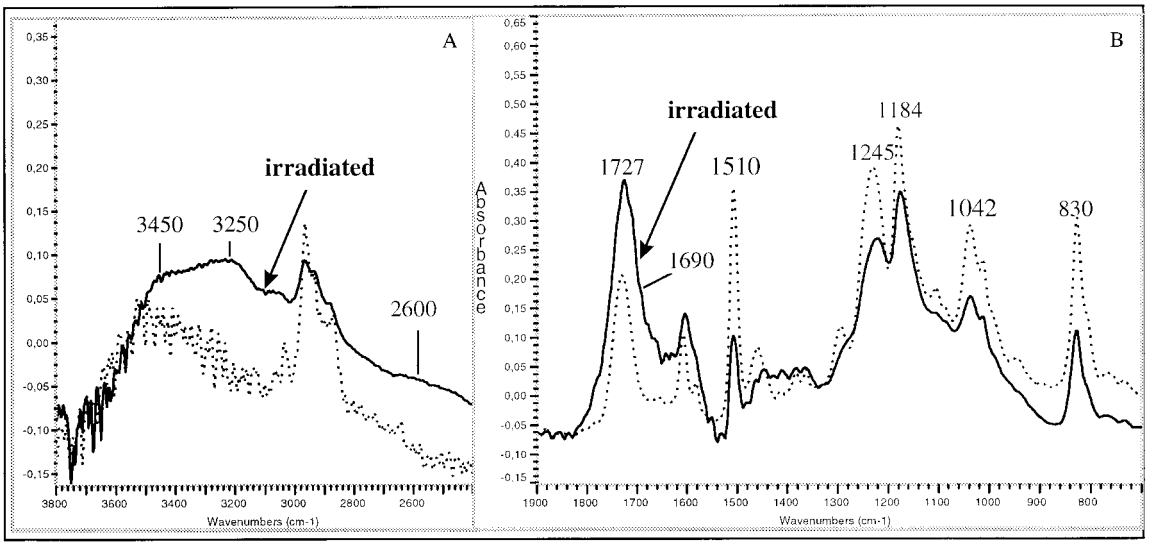


**Figure 10** ATR spectra of an EA sample, new (. . .), and after 160 h of irradiation (——).

cracking, etc.), which is responsible for the film's opacification. In spite of a multiplication of the spectrum obtained with aged film by a factor of 1.5, we note the very strong decrease of the aromatic bands (C═C at 1510 $cm^{-1}$; C—H at 830 $cm^{-1}$); the strong decrease of the bands characteristic of aromatic ethers (Φ—C—O at 1245 $cm^{-1}$) and of aliphatic ethers (1042 $cm^{-1}$), accompanied by a broadening of these bands; and, also, the strong decrease of the aliphatics [—$C(CH_3)_2$ at 1184 $cm^{-1}$ and $CH_3$ and $CH_2$ at 2966, 2933, and 2974 $cm^{-1}$]. Concurrently to the general decrease of all the initial bands of the polymer, we note the presence of particularly strong oxidation bands: the C═O band is intense and strongly shifted towards the low wave numbers (maximum at 1727 $cm^{-1}$ with important shoulders at 1710 and 1690 $cm^{-1}$), thus indicating a high concentration of acid products. In addition, the shoulders already observed by transmission at 1820, 1787, 1764, and 1724 $cm^{-1}$ are observed once again. In the hydroxyl region [Fig. 10(A)], besides a very broad band with a maximum at 3450 $cm^{-1}$ (attributed to aliphatic alcohols), we note the presence of a band of strong intensity with a maximum at 3250 $cm^{-1}$, probably corresponding to phenolic products, which are the classical photoproducts of aromatic polymers. In addition, we note the importance of the intensity of the broad acid OH band at 2600 $cm^{-1}$, which confirms the presence of high concentrations of acids at the surface.

Finally, in the C—O region [Fig. 10(B)], we note the emergence of 2 strong shoulders at 1225 $cm^{-1}$ (which may be attributed to phenols) and at 1180 $cm^{-1}$ (which may be attributed to aliphatic alcohols), as well as the increase of the absorbance around 1275 $cm^{-1}$ (which may be attributed to carboxylic acids).[12]

## Screening Effect

In order to assess the absorbance of the formed photoproducts, a UV absorption spectrum was obtained for a new film and, subsequently, for a film aged for 100 h (Fig. 11). The absorbance's evolution towards wavelengths well above 300 nm shows the formation during the degradation of strongly UV absorbing photoproducts. These

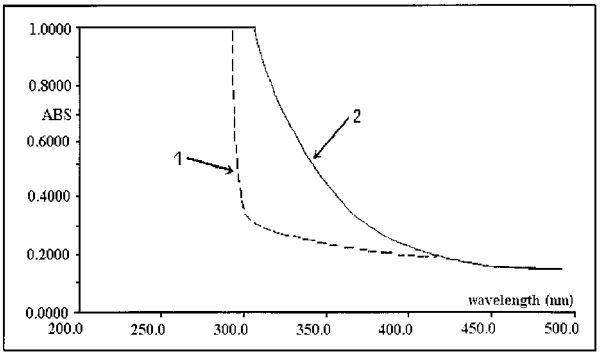


**Figure 11** UV absorption spectra of an EA film (1) nonirradiated and (2) after an irradiation time of 100 h.

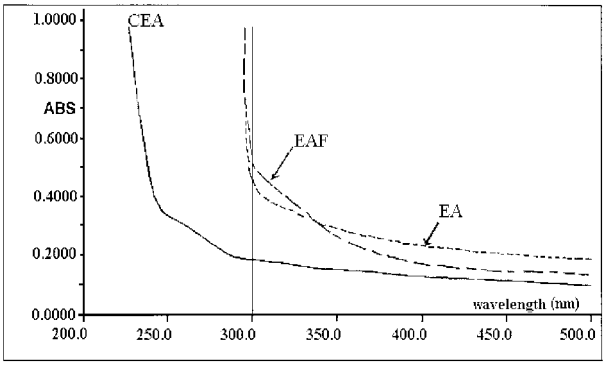


**Figure 12** UV absorption spectra of films of EA, EAF, and CEA systems.

products are probably responsible for the additional screening effect by UV absorption in the aged film's superficial layer. This effect and the absorption by the aromatic chromophores of the EA and EAF systems would partly explain the very heterogeneous degradation of the film and the formation of the thin, very strongly degraded surface layer that we have observed.

### UV Absorption Spectra and Degradation Mechanisms

In a first approach, Norrish-type mechanisms may be invoked to explain the disappearance of esters and the formation of numerous oxidized products as observed for EA and EAF systems. But for the same conditions of irradiation (UV light intensity and irradiation time), FTIR analysis didn't show any modification of the EAC (cycloaliphatic) system, which contains, however, a lot of ester groups in a similar configuration. The comparison of UV absorption spectra of the 3 new systems (Fig. 12) allows one to understand why the EAC system doesn't degrade under UV as both EA and EAF systems do. Indeed its aromatic-free structure doesn't absorb UV of wavelength longer than 300 nm. Thus, we could attribute the strong degradation of both aromatic systems to the absorption of UV light by aromatic structures followed by an intrinsic and/or induced degradation. Moreover, the shoulder observed in the EAF system UV absorption spectra (Fig. 12) may explain the rapid attack of the flexibilizer. Indeed, the comparison of UV absorption spectra of EA and EAF hardeners allowed us to attribute this shoulder to the flexibilizer contained in the EAF hardener. However, further consideration can be taken into account for the degradation mechanisms of EA and EAF systems. Some examples in the literature show in the case of aromatic chromophores that bond scissions may occur not only on the bonds directly linked to the ring but also on the bonds in the vicinity.[19] Figure 13 shows possible mechanisms for intrinsic degradation according to experimental observations and considering bonds dissociation energies.[20] In fact, the strong increase of hydroxyl bands confirms the formation of tertiary alcohols [a maximum around 3450 $cm^{-1}$; Fig. 10(A)] and phenols [a marked shoulder at 3250 $cm^{-1}$ in Figure 10(A) and 1225 $cm^{-1}$ in Fig. 10(B)]. The formation of conjugated ketones is more hypothetic; the slightly marked shoulder at 1690 $cm^{-1}$ (Fig. 10) might be characteristic for conjugated ketones but also for benzoic acid. Further analysis is necessary to confirm the formation of these products.

From the proposed mechanism can be drawn another explanation for the rapid degradation of the flexibilizer in the EAF system. Indeed, if radicals $CH_3^{\bullet}$ issued from reaction (1) [Fig. 13] will lead to the formation of a formaldehyde and, further, of a formic acid, radicals $—CH_2^{\bullet}$ from reaction 2(b) can give rise to different situations:

On one hand, it can give rise to the rapid propagation of oxidation in the EAF system, in the long linear chain constituted by the flexibilizer, by nibbling; on the other hand, it can give rise to a rapid annihilation of the oxidation processes in the EA system by formation of relatively stable phenol or quinone groups when reaching the aromatic group. Those mechanisms are depicted in Figure 14.

Another mechanism of induced photooxidation could explain the fast degradation of EA and EAF systems compared to the EAC. It is the oxidative attack of the hardener part of the EA and EAF molecules. Indeed, MTHPA (EA and EAF hardener) contains a double bond that is weakening the $—CH_2$ bond in its vicinity, although HHPA (EAC hardener) doesn't. This mechanism leads to carboxylic acids (1718 $cm^{-1}$) and conjugated ketones (1690 $cm^{-1}$) that we observe in FTIR on EA and EAF aged sample surfaces. As an induced oxidative one, this mechanism alone cannot explain the high degradation rate of EA and EAF systems compared to EAC, but it can account for the appearance of several observed degradation products. Finally, a last mechanism can be cited here as highly probable. This is the oxidative attack of the tertiary carbon–hydrogen bond of hardener cycles. This mechanism leads to conjugated ketones linked to an aliphatic segment that

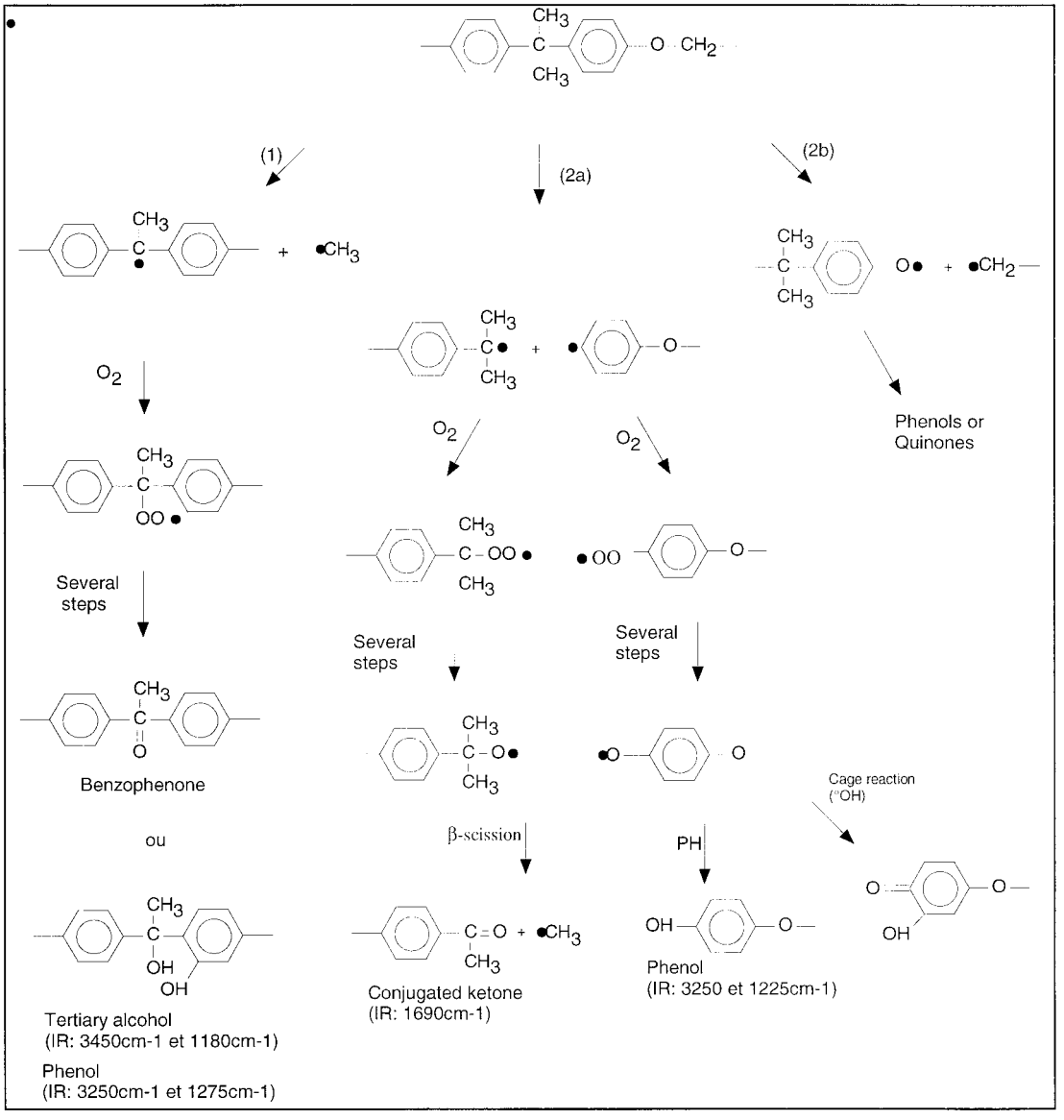


**Figure 13** Mechanisms for intrinsic photodegradation of EA and EAF systems.

will probably further degrade into low-molecular-weight by-products.[20]

## CONCLUSION

1. The 2 studied aromatic epoxy–anhydride systems are rapidly degraded by UV irradiation in the solar wavelength range. The structural modifications are considerable after only 50 h of irradiation.
2. The flexibilized system is degraded more rapidly during the first hours of exposure. We suppose a specific attack upon the flexibilizer's structural groups, the characteristic chemical functions of which disappear rapidly. Afterwards, this system continues to degrade, but only according to first-order kinetics, identically to the EA system.
3. The formed products are similar for the 2 systems. They react in a similar way to the different chemical treatments applied.
4. After 50 h of irradiation, the disappearance rate of aromatic groups does not depend on their initial concentration, whereas the increase of hydroxyl groups varies as the square root of time, which is generally ac-

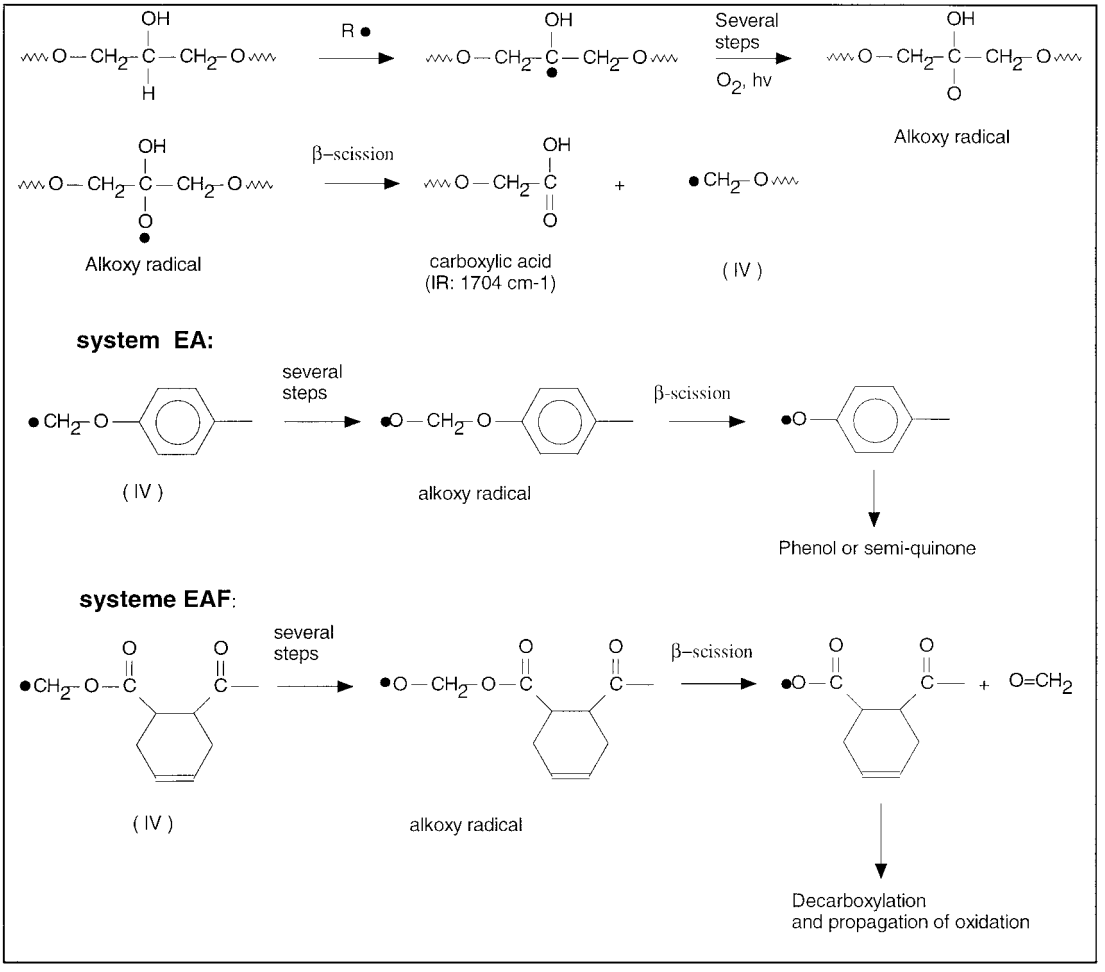


**Figure 14** Mechanisms for induced photooxidation showing the initiation of a nibbling degradation mechanism of an EAF system.

cepted for an oxidation process limited by the diffusion of oxygen in the material.

5. The considerable decrease of practically all the bands characteristic of the initial chemical functions, associated with the appearance of new, low-intensity bands, suggests the formation of a considerable quantity of volatile products.
6. The strong evolution of the UV absorption spectra towards higher wavelengths, indicating the formation of strongly UV absorbent products, suggests a rather marked screening effect. This effect, associated with the limitation of oxygen in the bulk of the material, is responsible for the very heterogeneous degradation of the films.
7. Norrish-type mechanisms may be involved to explain the disappearance of esters and the formation of numerous oxidized products, as observed for EA and EAF systems. But from the comparison with the cycloaliphatic system (aromatic free) EAC, we could attribute the strong degradation of both aromatic systems to the absorption of UV light by aromatic structures, followed by an induced photooxidative degradation. The fast degradation of the flexibilizer in the EAF system may be attributed either to a specific absorbance of UV light by the flexibilizer or to a nibbling phenomenon along the flexibilizer chemical structure (fast propagation of the induced photooxidation). Two other mechanisms of photooxidative degradation by a radical attack of the hardener cycles are cited, as they are highly probable. They could account for the formation of several photoproducts,

including carboxylic acids that we observed in our study by FTIR analysis.

These results as a whole indicate that ultraviolets should have a marked effect upon the electrical properties at the surface. The assessment of this impact on the functional properties of the epoxy resins used in electrical engineering will be the objective of the continuation of this work.

The authors thank the Clermont Ferrand Photochemistry laboratory for carrying out the SF4 treatment experiments and the acquisition of the corresponding spectra. They also thank J. L. Gardette, Research Director at the CNRS, and J. Verdu, Professor at ENSAM Paris, for fruitful discussions.

## REFERENCES

1. B. D. Gesner and P. G. Kelleher, *J. Appl. Polym. Sci.,* **13,** 2183 (1969).
2. P. G. Kelleher and B. D. Gesner, *J. Appl. Polym. Sci.,* **13,** 9 (1969).
3. N. Grassie, M. Guy, and N. H. Tennent, *Polym. Degrad. Stab.,* **13,** 249 (1985).
4. S. C. Lin, B. J. Bulkin, E. M. Pearce, *J. Polym. Sci.,* **17,** 3121 (1979).
5. V. Bellenger and J. Verdu, *J. Appl. Polym. Sci.,* **28,** 2677 (1983).
6. H. M. Le Huy, V. Bellenger, M. Paris, and J. Verdu, *Polym. Degrad. Stab.,* **35,** 77 (1992).
7. H. M. Le Huy, V. Bellenger, M. Paris, and J. Verdu, *Polym. Degrad. Stab.,* **35,** 171 (1992).
8. H. Nakagawa, S. Tsuge, and T. Koyama, *J. Anal. Appl. Pyrolysis,* **12,** 97 (1987).
9. B. Plage and H. R. Schulten, *Macromolecules,* **21,** 2018 (1988).
10. L. J. Bellamy, *The Infra-Red Spectra of Complex Molecules,* Methuen, London, 1958.
11. Nakanishi, *IR Absorption Spectroscopy*—Practical, 1962.
12. D. Lin Vien, N. B. Colthup, W. G. Fateley, and J. G. Grasseli, *The Handbook of Infrared and Raman Characteristic Frequencies of Organic Molecules,* Academic Press, New York, 1991.
13. G. C. Stevens, *J. Appl. Polym. Sci.,* **26,** 4259 (1981).
14. G. C. Stevens, *J. Appl. Polym. Sci.,* **26,** 4279 (1981).
15. J. F. Heacock, *J. Appl. Polym. Sci.,* **7,** 2319 (1963).
16. S. Wilheim and J. L. Gardette, *J. Appl. Polym. Sci.,* **51,** 1411 (1994).
17. A. Rivaton, *Polym. Degrad. Stab.,* **41,** 283 (1993).
18. J. Lacoste and D. J. Carlsson, *J. Appl. Polym. Sci.,* **30,** 493 (1992).
19. W. Schnabel and J. Kiwi, in *Aspects of Degradation and Stabilization of Polymers,* Elsevier, New York, 1978.
20. V. Ollier-Duréault, M.S. thesis, Joseph Fourier University of Grenoble, 1995.